



ARTICLE

Antimicrobial silicone rubbers based on photocatalytically active additives

Theresa Fischer  | Susana Suttor | Salma Mansi | Lucas Osthues |
Petra Mela 

Chair of Medical Materials and Implants,
Department of Mechanical Engineering
and Munich School of BioEngineering,
Technical University of Munich, Munich,
Germany

Correspondence

Theresa Fischer, Chair of Medical
Materials and Implants, Department of
Mechanical Engineering and Munich
School of BioEngineering, Technical
University of Munich, Boltzmannstr. 15,
85748 Garching b. München, Germany.
Email: theresa.fischer@tum.de

Funding information

AiF

Abstract

The modification of plastics to generate germ-reducing surface materials is a promising strategy to decrease nosocomial infections in hygiene-sensitive areas. In this paper, photocatalytically active nanoparticles were incorporated as additives, not as a coating, into silicone rubber matrix material to produce elastic antibacterial bulk materials. Samples with 5 wt% and 10 wt% of two different types of TiO₂ and ZnO were prepared and investigated. The thermal analysis of the developed materials showed a complete vulcanization of the developed materials and slight modifications of mechanical properties were found. Investigations of the surface of the materials indicated no changes in the wettability of the surfaces or in their fourier transform infrared spectrometer (FT-IR) spectra, suggesting no degradation of the developed material. The photocatalytic activity on the surface of the test samples was investigated by microbial tests with *Escherichia coli*, *Pseudomonas fluorescens*, and *Staphylococcus aureus* bacteria. Depending on the additive type and the test germs, the samples showed different intensities of a germ-reducing effect (up to >99,999%).

KEYWORDS

applications, crosslinking, irradiation, mechanical properties

1 | INTRODUCTION

Nosocomial infections have become a widespread problem.^{1,2} Contaminated surfaces, such as keyboards, water taps, door handles, and even seat cushions contribute to the transmission of hospital pathogens via direct contact by hospital staff and patients.^{3–7} The occurrence of nosocomial infections results in prolonged medical treatment time, residual damage and even deaths, and as a consequence, in overall rising healthcare costs.²

Compliance with strict hygiene regulations is regarded as the most important prevention measure while new

technologies are constantly being developed to further reduce the risk of nosocomial infections.^{8,9} Among these, antimicrobial plastics are proposed as contact surface materials^{10,11} to either kill (active effect) or inhibit the growth of microorganisms (passive effect).¹² Controlling surface properties such as free energy, topography, and charge result in a lower adhesion of germs,^{13,14} while the incorporation of biocidal elements such as metal nanoparticles into plastics is a strategy to obtain coatings with germ-reducing properties.^{15–19} Photocatalytically active substances have also been proposed as biocides.^{20–23} Their germicidal effect due to the reactive oxygen species (ROS) generated during the exposure to

This is an open access article under the terms of the Creative Commons Attribution License, which permits use, distribution and reproduction in any medium, provided the original work is properly cited.

© 2021 The Authors. *Journal of Applied Polymer Science* published by Wiley Periodicals LLC.

radiation,²⁴ which are responsible for the attack on organic structures and thus for the killing of germs.²⁵ Photocatalytically active substances have been mainly employed to create antimicrobial surface coatings.^{26–28} Such thin layers, however present several issues that can jeopardize their use as mean to create germ-reducing surfaces. Specifically, often not optimal adhesion to the underlying bulk material and the loss of the antimicrobial effect in case of surface damage are aspects to be considered.²⁹ Furthermore, antimicrobial additives have been used in combination with thermoplastic elastomers³⁰ and thermoplastic polymers^{31,32} and little to no effort to create antimicrobial elastomers has been reported. These materials, however, are relevant for covers like keypads, door handles or control panels. Therefore, in this work, we aimed at the development of an antimicrobial elastomeric compound material to be used as bulk material so that, in case of surface damage, the biocidal properties maintained. To this end we modified a high temperature vulcanizing (HTV) silicone rubber with photocatalytically active additives.

The compound was characterized by thermal, mechanical and surface analyses and tested with different bacteria (*Escherichia coli* [*E. coli*], *Pseudomonas fluorescens* (*P. fluorescens*), and *Staphylococcus aureus* [*S. aureus*]) at different irradiation times and after surface damage by mechanical ablation to evaluate the antimicrobial properties.

2 | EXPERIMENTAL

2.1 | Materials

HTV silicone rubber SILPURAN[®] 8020/40 with SILPURAN[®] curing agent M (Wacker Chemie AG, Germany) was used as bulk material. Three different solid powders were employed as photocatalytically active additives: (1) AEROXIDE[®] TiO₂ P25 (Evonik Industries AG, Germany) with average particle size of 21 nm, a powder density of 100–180 g/L, and 80:20 anatase to rutile crystal structure,^{33,34} (2) KRONOClean[®] 7000 (Krono) (KRONOS Inc., USA) with a particle size of 15 nm and a powder density of 350 g/L, a carbon fortified porous photocatalyst in anatase crystal modification), and (3) zinc oxide (ZnO) NANOTech[®] (Grillo Zinkoxid GmbH, Germany) with average particle size of 40 nm and a measured powder density of 290 g/L. The values of the particle size and the bulk density (except for ZnO) correspond to the respective data sheets.

2.2 | Preparation of test samples

Suspension of the nanoparticles in acetone were prepared in the w/w ratios indicated in Table 1 to facilitate their

TABLE 1 Ratio acetone/additive (w/w) for the incorporation of the particles into the matrix material

| Additive | Ratio acetone/additive |
|----------|------------------------|
| P25 | 3.4 |
| Krono | 1.0 |
| ZnO | 1.2 |

incorporation in the silicone and to prevent dispersion of the nanoparticles in the atmosphere. The amount of acetone for the different nanoparticles was determined iteratively to obtain a suspension that could be easily applied on the matrix as a layer containing a defined amount of particles. These 'working' suspensions correlated well to the powder densities, which were either indicated by the manufacturer or measured.

The modification of the silicone rubber was carried out using rolling process technologies.³⁵ To obtain the materials, 50 g of raw matrix material was rolled into a sheet (160 cm²) with a thickness of 2 mm (Figure 1(a)). The flat rolled silicone rubber mass was removed from the two-roll-mill and the particles were added by spreading the volume of suspension containing 0.5 g of particles (1% w/w) to form a thin layer (Figure 1(b)), followed by a continuous folding and rolling process (Figure 1(c)) for 30 minutes before repeating the sequence again to reach the target particle amount (either 5% w/w or 10% w/w). The final amount of additive was verified by weighing the produced sample after complete acetone evaporation.

Subsequently, the cross-linker was added (1.5% w/w) and the final mixture was rolled with a two-roll-mill into a sheet (Figure 1(a)–(c)) which was then pressed in a mold at 170°C and 50 bar for 25 min (figure 1(d)) and finally tempered for 4 h at 200°C (Figure 1(e)). Seven materials were produced with different additive amounts as summarized in Table 2.

The unmodified silicone served as control. Disk shaped specimens for the microbial tests were obtained by punching the foils with a 12 mm steel punch. Ring-shaped specimens with an outer diameter of 58 mm and an inner diameter of 50 mm were produced with a precision steel punch to investigate the mechanical properties (Figure 1(f)).

2.3 | Characterization

2.3.1 | Thermal analysis

Differential scanning calorimetry (DSC) was carried out with a DSC 204 cell NETSCH (NETSCH GmbH & Co. KG, Germany) according to DIN EN ISO 11357-5 in order to investigate the influences of the material modification on the curing process. The modified materials

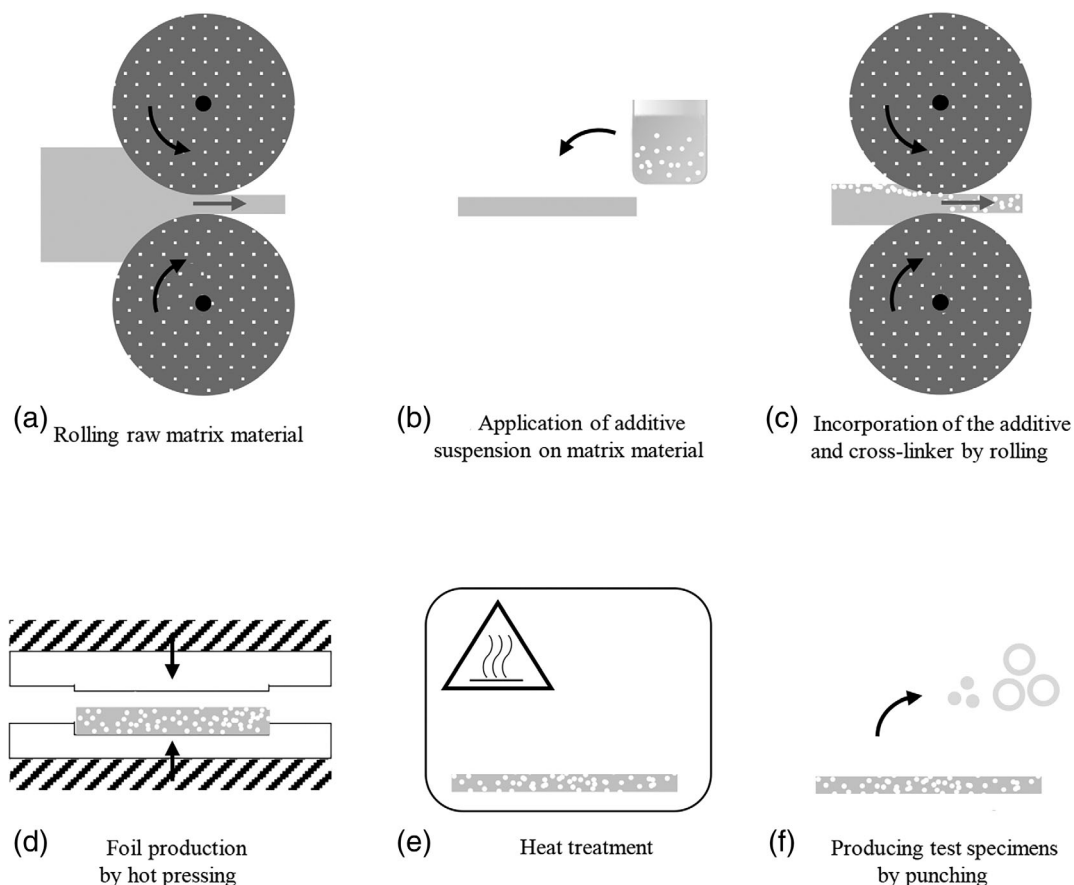


FIGURE 1 Production process of the different compounds (a)–(e) and of the test specimens (F)

TABLE 2 Overview of the produced composites

| Material | Additive | Weight percentage (%) |
|-----------|----------|-----------------------|
| Reference | — | 0 |
| ZnO_5 | ZnO | 5 |
| ZnO_10 | | 10 |
| P25_5 | P25 | 5 |
| P25_10 | | 10 |
| Krono_5 | Krono | 5 |
| Krono_10 | | 10 |

were filled into aluminum crucibles and placed in the DSC system. Together with an empty reference crucible, the samples were heated to 333.15 K with a heating rate of 5 K/min. The heat relative to the sample weight Q over temperature T and time t was recorded and the reaction enthalpy ΔQ was calculated.

2.3.2 | Mechanical analysis

Tensile strength σ_{max} and elongation at break ε_R were determined according to DIN 55304 with a tensile testing

machine (Zwick/Roell Z050, ZwickRoell GmbH & Co. KG, Germany) at a constant speed of $v = 500$ mm/min (sample number $n = 8$). The ring-shaped test specimens were placed on rotating rollers in order to avoid adhesion of the test samples to the rollers; a preload was not necessary.

2.3.3 | Surface analysis

Contact angle of the different composites was measured using the OCA 15EC contact angle measuring system (DataPhysics GmbH, Germany). All materials ($n = 15$) were investigated after an irradiation of 0 h, 2 h, and 100 h each at a wavelength of 365 nm with an intensity of 0.4–0.5 mW/cm². FT-IR ($n = 1$) with a scan number of 16 (Alpha II, Bruker Corporation, USA) was performed to detect degradation caused by irradiation.³⁶

2.3.4 | Microbial testing

The antimicrobial properties of the different materials were determined according to ISO 27447 and DIN EN 13697 with both gram-negative *E. coli* (IMG 1711) and

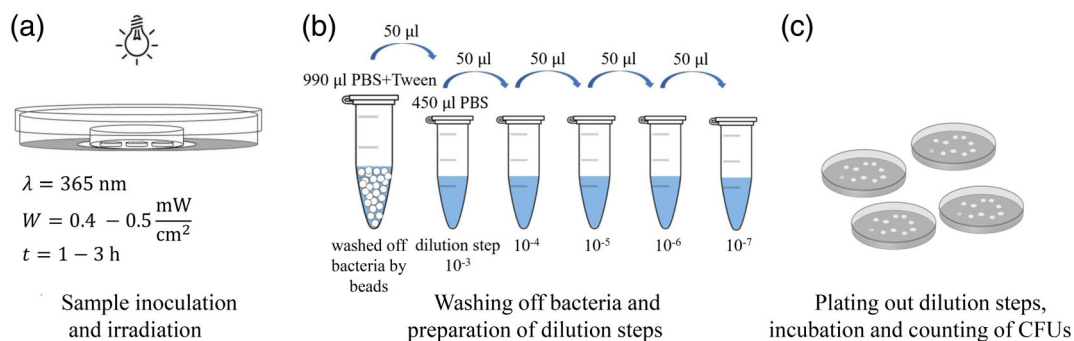


FIGURE 2 Microbial test procedure. (a) Inoculation and irradiation; (b) washing and dilution steps; (c) plating of dilution steps on agar plates, incubation and counting of colony forming units (CFUs) [Color figure can be viewed at wileyonlinelibrary.com]

P. fluorescens (ATCC 13252) and gram-positive (*S. aureus* [USA 300]) bacteria.

The basic microbial testing was carried out as follows: The samples were cleaned in an ultrasonic bath for 20 min and steam sterilized for 20 min at 121°C (Laboklav 25 V, SHP Steriltechnik AG, Germany). Subsequently, they were inoculated with 10 μ l germ suspension of 10⁸ colony forming units (CFU) per ml and treated as schematically shown in Figure 2(a).

The inoculated samples were positioned in a glass petri dish placed inside a bigger plastic petri dish containing a wet filter paper to preserve the moisture during the experiment. The samples were exposed to ultraviolet radiation at a wavelength of 365 nm with an intensity of 0.4–0.5 mW/cm² in order to elicit the photocatalytic effect of the nanoparticles. It was ensured that the material of the plastic petri dish was transparent to this radiation using a spectrophotometer (Agilent Technologies Inc., USA). After the irradiation period, the test samples were put into tubes filled with phosphate-buffered saline with 0.1 vol% polysorbate 80 (Tween) and glass beads. The remaining bacteria were washed off the test specimens by vortexing (equivalent to dilution step 10⁻², see Figure 2(b)). Subsequently, dilution steps up to 10⁻⁷ were prepared (Figure 2(b)). For each material, 100 μ l of each dilution step was plated on two separate agar plates. After an incubation of 24 h, the CFU on each agar plate were counted for numbers of CFU on the plate between 13 and 220 (Figure 2(c)), as advised by DIN EN 13697. The value remaining germs R_G in % was calculated for each material according to formula 2.1, where B_L = average value of CFUs on reference of all countable dilution steps and C_L = average value of CFUs on composites of all countable dilution steps.

$$R_G = \left(\frac{C_L}{B_L} \right) \cdot 100, \quad (2.1)$$

The error was computed according to error propagation (formula 2.2).³⁷

$$\delta R_G = \sqrt{\left(-\frac{100 \cdot C_L}{B_L^2} \right)^2 \cdot \delta B_L^2 + \left(\frac{100}{B_L} \right)^2 \cdot \delta C_L^2}, \quad (2.2)$$

The investigations of the germ reducing effect of the developed composites can be divided into two parts.

Influence of the irradiation period on antimicrobial properties

The irradiation period eliciting the antimicrobial effect against *E. coli* ($n = 6$) and *P. fluorescens* ($n = 4$) was set to 1 h, 2 h, and 3 h each at a wavelength of 365 nm with an intensity of 0.4–0.5 mW/cm² in order to investigate its influence on the intensity of the germ-reducing effect on all seven composites. In order to limit the number of experiments, the investigation of the antimicrobial effect against *S. aureus*, was carried out with only one percentage of each additive. DSC measurement, mechanical testing and antimicrobial activity against *E. coli* and *P. fluorescens* were considered in the selection of materials. The effect against *S. aureus* ($n = 4$) was investigated at an irradiation period of 2 h at a wavelength of 365 nm with an intensity of 0.4–0.5 mW/cm² on the reference material, ZnO 10 wt%, P25 10 wt% and Krono 5 wt%. The experiments were carried out as described above.

Effect of surface damage on antimicrobial properties

The antimicrobial activity in the bulk of the material was tested at an irradiation period of 2 h at a wavelength of 365 nm with an intensity of 0.4–0.5 mW/cm² and compared to the antimicrobial activity on the surface of the materials. For this, 0.25 mm of the complete surface of the composite materials with P25_10, ZnO_10 and Krono_5 was removed by laser cutting (Speedy 400 flexx, Trotec Laser GmbH, Austria) to expose the bulk of the material. Analogue to the first part of the microbial testing against *S. aureus*, only selected materials were used in the second part to reduce the number of experiments. The investigations were carried out as described above against the bacteria *E. coli* ($n = 4$), *P. fluorescens* ($n = 4$)

and *S. aureus* ($n = 4$) on the newly gained surface of the samples.

2.3.5 | Statistical analysis

The results of the mechanical evaluation and the contact angle measurement are presented as mean \pm SD. For comparison of mechanical strength, elongation at break and contact angle between the different materials and the different irradiation periods, Mann–Whitney-U-test were performed in Origin[®] with $\alpha = 0.05$ as not all data set were described by a normal distribution.

3 | RESULTS AND DISCUSSION

3.1 | Cross-linking reaction

The curing process of the reference material took place in a temperature interval of 120–150°C (Figure 3).

The curves of the ZnO composites are slightly shifted to lower temperature ranges compared to the reference, in contrast to the curves of all other composites, which are shifted to higher temperature ranges. Zinc oxide is an important inorganic additive used in the rubber industry as cure activator for the sulfur vulcanization and as curing agent for some elastomers containing specific reactive functional groups.³⁸ It is conceivable that the antimicrobial ZnO nanoparticles in our study additionally acted as curing activator and caused the vulcanization process to start at lower temperatures, with ZnO_10 result in a 10°C shift. The curves in Figure 3 indicate that for all the composites 25 min at 170°C were sufficient to complete the cross-linking. The curing process of the modified

materials compared to the reference showed a decreasing cross-linking enthalpy with increasing amount of additive, independent of the type of additive. The DSC measurements revealed the lowest cross-linking enthalpy for Krono_10, which corresponds to the lowest cross-linking density. A decreased cross-linking enthalpy was also shown in the case of a silicone modified with calcium phosphate nanoparticles,³⁹ as well as ZnO nanoparticles were added as fillers to obtain epoxy-polydimethylsiloxane composites for anticorrosion and hydrophobic coatings.⁴⁰ This can be explained by a lower cross-linking density due to the higher viscosity of the nanoparticle/elastomer mixture and the nanoparticles' steric hindrance, in agreement with Ramezanzadeh et al.,⁴¹ as it leads to a lower reaction of the functional groups of the matrix material. The KRONOClean[®] 7000 has the smallest particle size among the used additives, therefore more particles were present in the silicone matrix in comparison to the other composites, causing a higher steric hindrance.

3.2 | Mechanical properties

Figure 4(a) shows the tensile strength of the modified materials compared to the reference.

The statistical analysis of the tensile strength showed no differences compared to the reference material in case no irradiation was performed except for P25_10 and Krono_10. In case of the P25 the additive lead to an increase of the tensile strength. This statement concurs with Kong et al. who used additives as boron nitride and silicon nitride nanoparticles in silicone rubbers to increase the mechanical strength.⁴² The decreases of the tensile strength of Krono_10 confirmed the results of

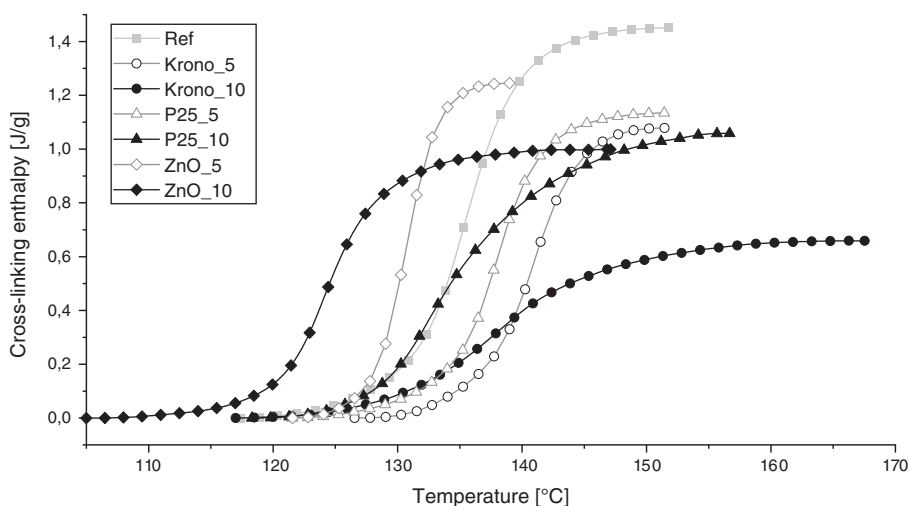


FIGURE 3 Cross-linking enthalpy of reference and composite materials as function of temperature. Increasing amounts of additive lead to decreasing enthalpies

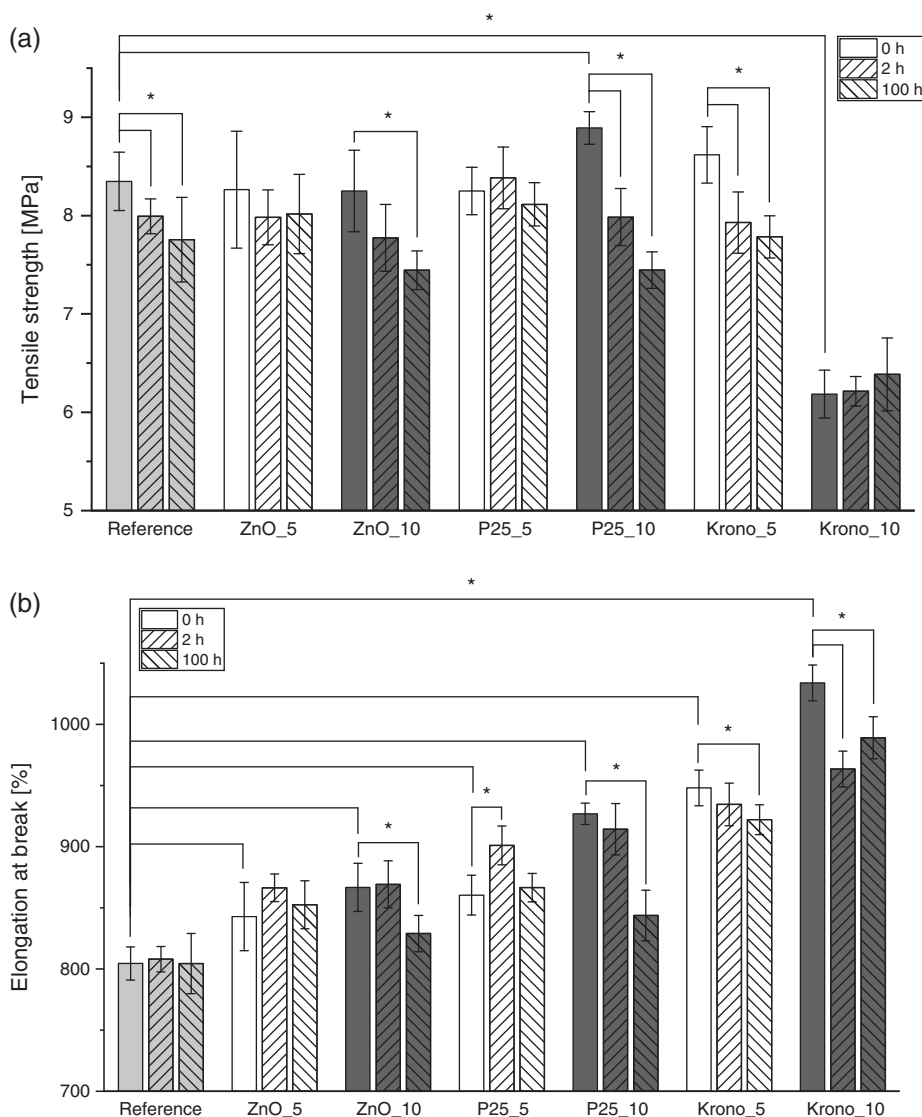


FIGURE 4 Mechanical properties of the reference and the modified materials. (a) tensile strength values ($n = 8$) after 0 h, 2 h, and 100 h of irradiation; (b) elongation at break values ($n = 8$) after 0 h, 2 h and 100 h irradiation. Significant changes of the mechanical properties of Krono 10 wt% indicate an insufficient cross-linking. Increasing irradiation period leads to decreasing mechanical values and suggest an accelerated degradation. * indicates statistical significance ($p < 0.05$)

the DSC measurement and thus an insufficient cross-linking at Krono_10 can be assumed.

The tensile strength of the reference material, ZnO_10, P25_10 and Krono_5 indicates statistically decreasing values with an increasing irradiation period. As decreasing tensile strength can be a sign of degradation of plastics caused by UV irradiation.

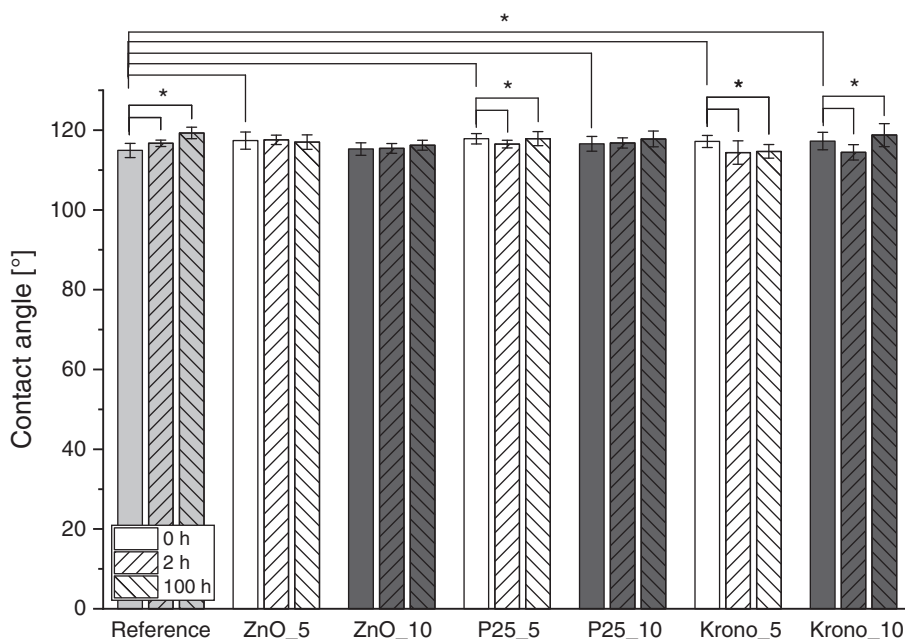
Earlier studies said that nanoparticle used as additives in liquid silicone rubbers (LSR) can increase tensile strength as nanoparticles act as additional physical crosslinking sites.⁴³ Wang et al. could confirm the enhancement of the tensile strength, but also found that a poor distribution of the nanoparticles lead to agglomerates that have a negative impact on the tensile strength of the used silicone fluid.⁴⁴ In case of this work a poor distribution of the additive can be assumed in Krono_10 taking the results of the tensile strength into account. The investigation of the distribution of the material with conventional methods like SEM-EDX (SEM stands for

scanning electron microscope-EDX stands for energy dispersive X-ray spectroscopy) was not possible as the material was damaged during the measurements.

The measured values of elongation at break are shown in Figure 4(b). The elongation at break showed statistically higher values for all composites compared to the reference at 0 h of irradiation. This enhancement of the elongation at break agrees also with the investigations of Kong et al.⁴² The material with 10 wt% Krono indicated the greatest contrast to the reference: the median of the elongation at break increased by up to 20% compared to the reference. The influence of 100 h irradiation result in significant lower values compared to 0 h irradiation: ZnO_10, P25_10, Krono_5 and Krono_10 show a decreasing elongation at break with higher irradiation period. A faster degradation of the material because of the emerging radicals can be assumed.

In summary, the tensile strength of the composites showed only slight differences compared to the

FIGURE 5 Contact angles ($n = 15$) of the reference and the modified materials after 0 h, 2 h, and 100 h irradiation. The means including their *SDs* are shown. The values were all measured in a range of 114–119°. * indicates statistical significance ($p < 0.05$)



reference material in case no irradiation was performed while the elongation at break increases. The irradiation of the materials can lead to a decrease of the mechanical values, but, except for the high tensile strength loss of Krono_10, the mechanical values change within a range that should have no influence on the application as contact surfaces like keyboards, handle bars and light switches.

3.3 | Surface analysis

Figure 5 visualizes the contact angles of the reference and the different composites after 0 h, 2 h, and 100 h of irradiation.

The means of the determined contact angles were all measured within a range of 114–119°. The non-irradiated composites showed a significant increase and thus a more hydrophobic surface compared to the reference. This increase of the contact angle by just about 2° can be explained by a rougher surface of the test specimens due to the mold used in the manufacturing process.⁴⁵ Since the nanoparticles were incorporated into the matrix material and thus completely surrounded by the silicone elastomer, the increase of the contact angle of the nonirradiated composites is not due to the additive. The unchanged contact angle of the non-irradiated composite ZnO_10 thus is in accordance with the expectations. During photocatalytic activation, oxygen vacancies occur in the structure of the photocatalyst titanium dioxide where water molecules can bind and lead to an absorption of OH groups that results in a higher free

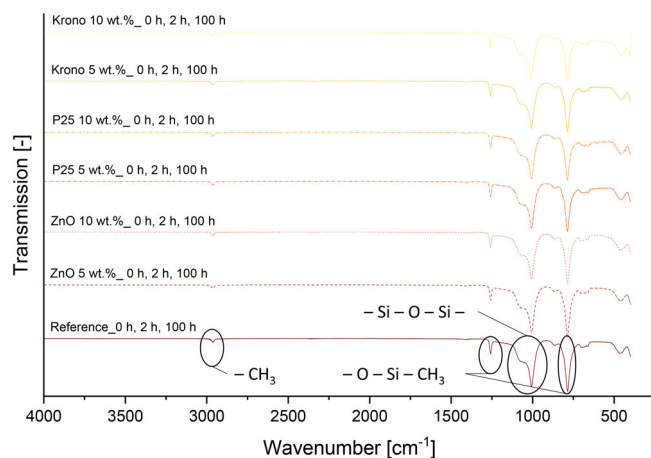


FIGURE 6 FT-IR spectra of the reference and the composites materials after 0 h, 2 h and 100 h of irradiation. The spectra within a composite of different irradiation periods are displayed stacked on top of each other, no differences could be detected [Color figure can be viewed at wileyonlinelibrary.com]

surface energy.⁴⁶ Huppmann et al. could prove this by creating hydrophilic plastic surfaces using TiO₂ nanoparticles as additives in thermoplastics.⁴⁷ This trend could be confirmed in parts in our studies. A significant reduction of the contact angle after 2 h of irradiation was measured on the composite surfaces of P25_5, Krono_5 and Krono_10. As it would be expected that, contrary to the results, both an increasing amount of additive and a prolonged irradiation period should enhance this effect, the occurrence of the phenomenon “hydrophobic recovery” should be considered: the hydrophobic recovery

causes a change in location of the hydrophilic functional groups from the surface into the bulk of the composites⁴⁸ and thus prevents the decrease of the contact angle. A change of the contact angles of the ZnO-composites due to the irradiation was not expected. A possible explanation for the significant increase of the contact angle of the reference material with increasing irradiation as well as of the composites P25_5 and Krono_10 after 100 h could be a changed surface structure due to UV radiation and thus a sign of degradation.⁴⁹ As the results of the tensile testing indicated a degradation of the composite materials at least after an irradiation of 100 h, surface analyses were carried out to obtain further information on the aging of the composites. Figure 6 shows the FT-IR spectra of the reference material and the composites after 0 h, 2 h, and 100 h irradiation.

The spectra within a composite of different irradiation periods are displayed stacked on top of each other. The peak between the wavenumbers 2965 cm^{-1} and 2960 cm^{-1} indicates a C–H₃ bonds and thus an organic polymer chain end.⁵⁰ The other three main bands of

the spectra ($1260\text{--}1254\text{ cm}^{-1}$, $1130\text{--}960\text{ cm}^{-1}$, $810\text{--}755\text{ cm}^{-1}$), highlighted in Figure 6, correspond to the silicone polymer chain. In the region of $1130\text{--}960\text{ cm}^{-1}$ Si–O–Si– bonds show a very strong infrared band.^{51,52} The –O–Si–CH₃ group is recognized by a sharp band at about $1260\text{--}1254\text{ cm}^{-1}$ together with a strong band in the range $810\text{--}755\text{ cm}^{-1}$, whereas both regions can refer to the molecule –O–Si–(CH₃)₃ as well as to –O₃–Si–CH₃.⁵¹ If the material degrades after irradiation, a change in the intensity of the bands can be expected. Since polymer chains break as a result of degradation, the peak of C–H₃ and the bands of O–Si–CH₃ as well as –Si–O–Si– should decrease. Huh et al. found a decrease of these peaks after an irradiation period of 2000 h, however, it was observed that the decreasing rate of C–H₃ and –Si–CH₃ bond is higher than that of –Si–O–Si– binding.⁵³ No differences in our spectra could be detected. Changes of the wettability of a surface (Figure 5) should also provide information about the resistance and the degradation of the materials.⁵⁴ Thus, the assumption of degradation

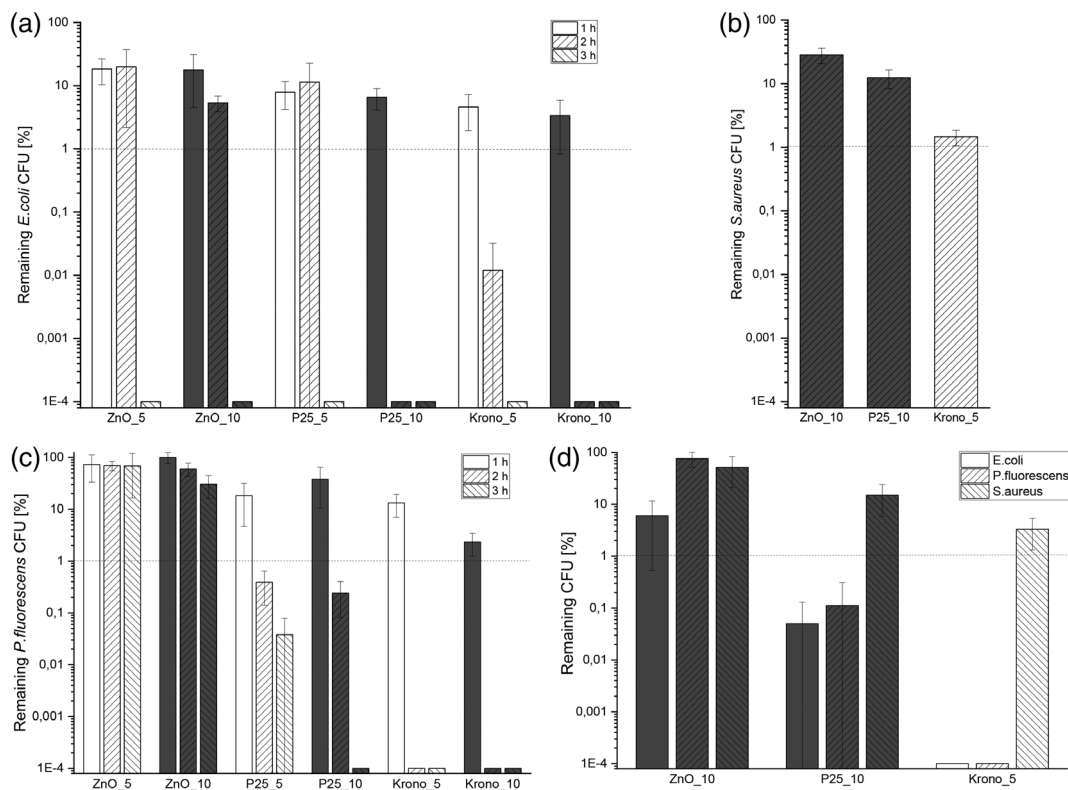


FIGURE 7 Antibacterial surface activity of the modified materials against gram-negative *Escherichia coli* ($n = 6$) (a), gram-negative *Pseudomonas fluorescens* ($n = 4$) (b) and gram-positive *S. aureus* ($n = 4$) (c) at different irradiation periods as well as the antibacterial activity in the bulk of the material at an irradiation period of 2 h ($n = 4$) (d). The dotted line represents a reduction of two log-steps and thus an antimicrobial effect. An increasing germ-reducing effect was observed with an increasing additive amount and higher irradiation period. Gram-negative bacteria showed a higher reduction of colony forming units compared to gram-positive bacteria. The germ-reduction in the bulk of the material corresponds with the results measured on the surface of the composites

could not be confirmed by examination of the wettability and FT-IR method.

3.4 | Germ-reducing effect

Figure 7 shows the measured antibacterial surface activity *E. coli* (Figure 7(a)), *P. fluorescens* (Figure 7(c)) and *S. aureus* (Figure 7(b)) at different irradiation periods as well as the antibacterial activity in the bulk of the material against these bacteria (Figure 7(d)).

The germ-reducing effect of all composites was tested against *E. coli* and *P. fluorescens* on samples that were irradiated 1 h, 2 h, and 3 h to cause the germ-reducing effect. According to the standard JIS Z 2801 a germ-reduction >2 log steps (99.00%) may be referred to as an antimicrobial effect. Looking at Figure 7(a), all composites represent an antimicrobial surface at a irradiation period of 3 h. Reducing the irradiation to 2 h result in a reduction of the germ-killing effect, but the composites ZnO_10, P25_10, Krono_5 and Krono_10 still work as antimicrobial surfaces. At an irradiation period of 1 h none of the composite surfaces appear as antimicrobial. Pal et al. investigated the influence of irradiation period and different loadings of P25 impregnated on membrane filters against *E. coli* and found the same effect: an increasing germ-reducing effect with an increasing irradiation period as well as an increasing additive amount.⁵⁵ This trend could also be confirmed against the germ *P. fluorescens*, however, our investigations indicate a higher or an equal antimicrobial activity against *E. coli* than against *P. fluorescens*. On closer examination of the various additives, TiO₂-composites showed a higher germ reducing effect than ZnO-composites, independent of the germ type. ZnO and TiO₂-coatings on PET/PBS blends were tested by Threepopnatkul et al. regarding their antimicrobial activity. The experiments delivered the same trend: the TiO₂-coating had a higher germ-reduction than the ZnO-coating.⁵⁶ The differences in the antimicrobial effect of the TiO₂-composites can be explained by the differences in the crystal modification of P25 and Krono. P25 is a mixture of anatase and rutile phases, as Krono consists of C-modified Anatase. Compared to anatase or rutile in pure phase, the mixed-phase TiO₂ is said to have a higher photocatalytic activity.⁵⁷ However, investigations of Xie et al. show that C-modifying is an effective way to improve the photocatalytic activity of TiO₂ for decomposition of organic compounds.⁵⁸ In case of our experiments C-modified Anatase (Krono) had the highest germ-reducing effect independent of the germ type and thus the best photocatalytic activity than the mixed-phase TiO₂ (P25). Considering the microbial investigations against gram-negative germs, we decided to conduct

further experiments with high additive amount composites to reach a maximum of the antimicrobial effect. In case of the additive Krono, we chose Krono_5, as the thermal and mechanical investigations suggest insufficient curing of the 10 wt% composite. The analysis against the gram-positive bacteria *S. aureus* (Figure 7(c)) showed a lower antibacterial activity compared to the gram-negative bacteria at an irradiation period of 2 h. The induced ROS of the photocatalyst kill germs by attacking the cell membrane²⁵ that is thicker in case of gram-positive bacteria. Consequently, the germ-reducing effect against gram-negative bacteria is higher than against gram positive germ at the same photocatalytic activity, as several studies confirm.^{55,56,59} Figure 7(d) visualizes the second part of the microbial investigations, the antibacterial activity in the bulk of the different composites at an irradiation period of 2 h. The trend of the values of the germ-reducing effect agrees with the trends measured on the surface: an increasing germ-reducing effect with an increasing additive amount as well as a higher antimicrobial activity against gram-negative bacteria than against the gram-positive *S. aureus*. This correspondence of the results on the surface and in the bulk of the composites proves that the antibacterial effect is maintained even on damaged surfaces.



4 | CONCLUSION

In this paper we show the fabrication and the analysis of an antibacterial silicone rubber. The usage of photocatalytically active fillers (TiO₂ and ZnO) led to a germ-reducing elastomer that has its effect not only on the surface of the material but also in the bulk. The developed composite Krono_5 showed the best results in our paper. Regarding the tensile strength of this composite, no statistical changes compared to the reference material could be detected, independent of the irradiation period. A germ-reduction >5 log steps is possible even on damaged surfaces. Therefore, an application of these materials as covers for door handles, keypads or control panels in public areas can reduce the risk of (nosocomial) infections.

ACKNOWLEDGMENTS

This work was funded by AiF (IGF-Vorhaben 19079 N/2). The authors gratefully thank the Chair of Organic Chemistry II, Technical University of Munich, Germany for their infrastructure and instrument support for this project. Open Access funding enabled and organized by Projekt DEAL.

ORCID

Theresa Fischer  <https://orcid.org/0000-0003-3137-8287>
Petra Mela  <https://orcid.org/0000-0001-6503-076X>

REFERENCES

- [1] P. Gastmeier, C. Geffers, *Deutsch. Med. Wochenschr.* **2008**, *133*, 1111.
- [2] J. P. Burke, *N. Engl. J. Med.* **2003**, *348*, 651.
- [3] S. Bures, J. T. Fishbain, C. F. Uyehara, J. M. Parker, B. W. Berg, *Am. J. Infect. Control* **2000**, *28*, 465.
- [4] G. A. Noskin, P. B. Bednarz, T. Suriano, S. Reiner, L. R. Peterson, *Am. J. Infect. Control* **2000**, *28*, 311.
- [5] J. A. Otter, S. Yezil, J. A. G. Salkeld, G. L. French, *American Journal of Infection Control* **2013**, *6*, 6.
- [6] W. A. Rutala, M. S. White, M. F. Gergen, D. J. Weber, *Infect. Control Hosp. Epidemiol.* **2006**, *27*, 372.
- [7] K. Zachary, P. S. Bayne, V. J. Morrison, D. S. Ford, L. C. Silver, D. C. Hooper, *Infect. Control Hosp. Epidemiol.* **2001**, *22*, 560.
- [8] B. Jansen, W. Kohlen, *Krankenhaushygiene up2date* **2008**, *3*, 201.
- [9] *Global Action Plan on Antimicrobial Resistance*, World Health Organization, Genf, Schweiz **2015**.
- [10] A. Jain, A. S. Duvvuri, S. Farah, N. Beyth, A. J. Domb, W. Khan, *Adv. Healthcare Mater.* **2014**, *3*, 1969.
- [11] V. T. H. Pham, C. M. Bhadra, V., K. Truong, R. J. Crawford, Designing antibacterial surfaces for biomaterials implants. in *Antibacterials Surfaces*, Vol. 89-112 (Eds: E. P. Ivanova, R. J. Crawford), Springer International Publishing, Switzerland: London **2015**.
- [12] V. Sedlarik, in *Antimicrobial modifications of polymers, in Biodegradation - Life of Science* (Eds: R. Chamy, F. Rosenkranz), IntechOpen, London, United Kingdom **2013**.
- [13] D. Ochs, B. Wirkstoffe, in *Handbuch Kunststoff-Additive* (Eds: R.-D. Maier, M. Schiller), Carl Hanser Verlag GmbH & Co. KG, München, Germany **2016**, p. 1139.
- [14] I. Francolini, G. Donelli, F. Crisante, V. Taresco, A. Piozzi, Antimicrobial Polymers for Anti-biofilm Medical Devices: State-of-Art and Perspectives. in *Biofilm-based Healthcare-associated Infections* (Ed: G. Donelli), Springer, Cham **2015**, p. 93.
- [15] D. Campoccia, L. Montanaro, C. R. Aricola, *Biopolymers* **2013**, *34*, 8533.
- [16] J. S. Kim, E. Kuk, K. Yu, J. Kim, *Nanomed.: Nanotechnol., Biol. Med.* **2007**, *3*, 95.
- [17] X. Li, S. M. Robinson, A. Gupta, K. Saha, Z. Jiang, D. F. Moyano, A. Sahar, M. A. Riley, V. M. Rotello, *ACS Nano* **2014**, *8*, 10682.
- [18] P. Prema, R. Raju, *Biotechnol. Bioprocess Eng.* **2009**, *14*, 842.
- [19] K. Zheng, M. I. Setyawati, D. T. Leong, J. Xie, *ACS Nano* **2017**, *11*, 6904.
- [20] H. A. Foster, I. B. Ditta, S. Varghese, A. Steele, *Appl. Microbiol. Biotechnol.* **2011**, *90*, 1847.
- [21] A. Khataee, G. A. Mansoori, *Nanostructured Titanium Dioxide Materials - Properties, Preparation and Applications*, World Scientific Publishing Co. Pte. Ltd, Singapur **2012**.
- [22] K. Gold, B. Slay, M. Knackstedt, A. K. Gaharwar, *Adv. Ther.* **2018**, *1*, 1700033.
- [23] J. Bogdan, J. Zarzyńska, J. Pławińska-Czarnak, *Nanoscale Res. Lett.* **2015**, *10*, 309.
- [24] A. Fujishima, K. Hashimoto, T. Watanabe, *TiO₂ photocatalysis: fundamentals and applications*, Tokyo Bkc, Tokio **1999**.
- [25] J. Winkler, *Titandioxid: Produktion, Eigenschaften und effektiver Einsatz. Vol. 2*, Vincentz Network GmbH & C, Hannover **2013**.
- [26] P. Muranyi, C. Schraml, J. Wunderlich, *J. Appl. Microbiol.* **2010**, *108*, 1966.
- [27] J. C. Yu, W. Ho, J. Lin, H. Yip, P. K. Wong, *Environ. Sci. Technol.* **2003**, *37*, 2296.
- [28] C. Rapp, A. Baumgärtel, L. Artmann, M. Eblenkamp, *Curr. Dir. Biomed. Eng.* **2016**, *2*, 43.
- [29] E. Richter, O. Schacker, Oberflächenaktive Zusatzstoffe. in *Handbuch Kunststoff-Additive* (Eds: R.-D. Maier, M. Schiller), Karl Hanser Verlag, München **2016**, p. 583.
- [30] M. Pittol, D. Tomacheski, D. N. Simoes, V. Ribeiro, *Mater. Res.* **2017**, *20*, 1266.
- [31] C. Radheshkumar, H. Münstedt, *React. Funct. Polym.* **2006**, *66*, 780.
- [32] N. Thokala, C. Kealey, J. Kennedy, D. Brady, *Mater. Sci. Eng., C* **2017**, *78*, 1179.
- [33] R. I. Bickley, T. Gonzalez-Carreno, J. S. Lees, R. J. D. Tilley, L. Palmisano, *J. Solid State Chem.* **1991**, *92*, 178.
- [34] B. Ohtani, O. O. Prieto-Mahaney, D. Li, R. Abe, *J. Photochem. Photobiol., A* **2010**, *216*, 179.
- [35] T. Fischer, M. Ahrens, M. Eblenkamp, *AIP Conf. Proc.* **2019**, *2139*, 180001.
- [36] W. Grellmann, S. Seidler, in *Prüfung physikalischer Eigenschaften, in Kunststoffprüfung* (Eds: W. Grellmann, S. Seidler), Carl Hanser Verlag, München **2005**.
- [37] R. Waldi, *Statistische Datenanalyse - Grundlagen und Methoden für Physiker*, Springer-Verlag GmbH, Berlin **2015**.
- [38] J. S. Dick, R. A. Annicelli, *Rubber Technology: Compounding and Testing for Performance*, Vol. 2, Carl Hanser Verlag, München **2009**.
- [39] O. F. Bareiro, L. A. Santos, *Mater. Sci. Forum* **2012**, *727-728*, 1175.
- [40] S. Ammar, K. Ramesh, B. Vengadaesvaran, S. Ramesh, A. K. Arof, *Prog. Org. Coat.* **2016**, *92*, 54.
- [41] B. Ramezanzadeh, M. M. Attar, M. Farzam, *Progress Org. Coat.* **2011**, *72*, 410.
- [42] S. M. Kong, M. Mariatti, J. J. C. Busfield, *J. Reinf. Plast. Compos.* **2011**, *30*, 1087.
- [43] M. W. Simon, K. T. Stafford, D. L. Ou, *J. Inorg. Organomet. Polym. Mater.* **2008**, *18*, 364.
- [44] L. Wang, Q. Liu, D. Jing, S. Zhou, *J. Dentist.* **2014**, *42*, 475.
- [45] M. Nosonovsky, B. Bhushan, *Microelectron. Eng.* **2007**, *84*, 382.
- [46] A. Fujishima, X. Zhang, D. A. Tryk, *Surf. Sci. Rep.* **2008**, *63*, 515.
- [47] T. Huppmann, S. Yatsenko, S. Leonhardt, E. Krampe, I. Radovanovic, M. Bastian, E. Wintermantel, *AIP Conf. Proc.* **2014**, *1593*, 440.
- [48] M. J. Owen, P. J. Smith, *J. Adhes. Sci. Technol.* **2012**, *8*, 1063.
- [49] K. Reincke, B. Langer, S. Döhler, U. Heuert, W. Grellmann, *KGK Kautschuk Gummi Kunststoffe* **2014**, *67*, 60.
- [50] T. Fox, Infrarot- und Raman-Spektren. in *Spektroskopische Methoden in der organischen Chemie* (Eds: S. Bienz, L. Bigler, T. fox), Georg Thieme Verlag, Stuttgart **2016**.
- [51] P. Launer, B. Arkles, Infrared analysis of organosilicon compounds. in *Silicon Compounds: Silanes & Siloxanes* (Eds: B. Arkles, G. L. Larson), Gelest Inc, Morrisville, Pennsylvania, United States **2013**, p. 175.
- [52] M. J. Owen, P. R. Dvornic, *Silicone Surface Science*, Springer Netherlands, Dordrecht **2012**.
- [53] C.-S. Huh, B.-H. Youn, S.-Y. Lee, *Proc. 6th Int. Conf. Prop. Appl. Dielectr. Mater.* **2000**, *1*, 367.

- [54] W. Grellmann, S. Seidler, G. Busse, Zerstörungsfreie Kunststoffprüfung. in *Kunststoffprüfung* (Eds: W. Grellmann, S. Seidler), Carl Hanser Verlag, Wien **2005**, p. 465.
- [55] A. Pal, S. O. Pehkonen, L. E. Yu, M. B. Ray, *J. Photochem. Photobiol., A* **2007**, *186*, 335.
- [56] P. Threepopnatkul, C. Wongnarat, W. Intolo, S. Suato, C. Kulsetthanchalee, *Energy Proc.* **2014**, *56*, 102.
- [57] J. Yan, G. Wu, N. Guan, L. Li, Z. Li, X. Cao, *Phys. Chem. Chem. Phys.* **2013**, *15*, 10978.
- [58] Y. Xie, X. Zhao, Y. Chen, Q. Zhao, Q. Yuan, *J. Solid State Chem.* **2007**, *180*, 3576.
- [59] H. K. Tsou, P. Y. Hsieh, in *Application of Titanium Dioxide* (Ed: M. Janus), IntechOpen, London, United Kingdom **2017**.

How to cite this article: T. Fischer, S. Suttor, S. Mansi, L. Osthues, P. Mela, *J Appl Polym Sci* **2021**, *138*(46), e51352. <https://doi.org/10.1002/app.51352>